

Hydrodynamics of slip wedge and optimization of surface slip property

MA GuoJun, WU ChengWei[†] & ZHOU Ping

State Key Laboratory of Structural Analysis for Industrial Equipment, Department of Engineering Mechanics, Dalian University of Technology, Dalian 116024, China

The hydrodynamic load support generated by a slip wedge of a slider bearing was studied. The surface slip property was optimized so that a maximum hydrodynamic load support could be obtained. A multi-linearity method was given for the slip control equation of two-dimensional (2-D) wall slip. We investigated 2-D wall slip and the hydrodynamics of a finite length bearing with any values of the surface limiting shear stress. It was found that the hydrodynamic effect of the slip wedge is greater than the traditional geometrical convergent-wedge. Even though the geometrical gap is a parallel or divergent sliding gap, the slip wedge still gives rise to a very big hydrodynamic pressure. The optimized slip wedge can give rise to a hydrodynamic load support as high as 2.5 times of what the geometrical convergent-wedge can produce. Wall slip usually gives a small surface friction.

wall slip, slip wedge, limiting shear stress, optimization

The boundary condition of fluid flow over a solid surface is one of the important factors to determine the hydrodynamic effect of the fluid film flowing in a solid surface gap with relative motion. The classical fluid mechanics and lubrication mechanics are based on the same assumption: no slip occurs at the interface of solid and fluid, i.e., the so-called no-slip boundary condition. This assumption has been widely used in various macro-engineering designs and experiments. Almost all the computations of macrofluid mechanics and rheology tests are based on this assumption. Based on the no-slip assumption, the famous Reynolds equation, a foundation of lubrication theory, was set up in 1886^[1]. The classical Reynolds theory shows that a geometrical convergent wedge (convergent gap) is the first important condition for the generation of hydrodynamic pressure of a steady sliding gap. No hydrodynamic pressure can be built up in either a parallel or a divergent gap. For over one hundred years since Reynolds theory came out, the convergent wedge has been a precondition for the design and manufacture of all the hydrodynamic

Received December 29, 2005; accepted November 21, 2006

doi: 10.1007/s11433-007-0034-x

[†]Corresponding author (email: cwwu@dlut.edu.cn)

Supported by the National Natural Science Foundation of China (Grant Nos. 10421002, 10332010 and 10672035), the National Basic Research Program of China (Grant No. 2006CB601205), and the Specialized Research Fund for the Doctoral Program of Higher Education of China (Grant No. 2006014007)

bearings. It is also one of the important foundation stones of lubrication mechanics.

Cameron^[2] presented a concept of the temperature-viscosity wedge in 1958. He found that if the temperature of the fluid film changed in the gap direction, there was still a considerable hydrodynamic load support even though for a parallel sliding gap. However, due to its small hydrodynamic effect, the temperature-viscosity wedge has been hardly used in engineering design.

With the continuous progress of the nano-measurement techniques during recent years, a nanoscale measurement is possible for the wall slip (boundary slip)^[3–8] of fluid flow over a solid surface. Wall slip is paid much attention to and is considered as one of the new directions in mechanics research^[9,10]. Experiments showed that wall slip takes place not only at a hydrophobic surface but also at a hydrophilic surface. When the surface shear stress reaches a critical (limiting) value, wall slip occurs; otherwise no slip occurs^[6–9]. If the surface is ultrahydrophobic, the critical shear stress for wall slip to occur is so small that the surface looks like a perfect slip surface^[9,11]. Besides the experimental observations, molecular dynamics (MD) simulation also confirmed that a slip occurs on the interface of solid and fluid^[12,13]. Wu et al.^[11,14,15] developed a limiting shear stress model to analyze the wall slips in one-dimensional gap flow and spherical surface squeeze film flow. A striking agreement exists between theoretical prediction and the experiment. Spikes^[16,17] studied the mechanics behavior of a half-wetted bearing. He found that wall slip can decrease the friction drag, but gives rise to a low hydrodynamic load support as well. All the studies mentioned above were based on the convergent wedge, the basic frame of the classical Reynolds theory. It was found that wall slip causes the hydrodynamic effect to decrease. Therefore, those studies showed that wall slip has a negative contribution to the generation of the hydrodynamic pressure. Salant and Fortier^[18] conducted a numerical analysis of a finite slider bearing with a heterogeneous slip/no-slip surface by means of a modified slip length model^[19] and found that such a bearing can provide a high load support but a low friction drag. However, they met an instability problem in the numerical solution when the critical shear stress is nonzero and thus concluded that the bearing operates in an unstable state.

This paper studies the hydrodynamic load support generated by the slip wedge based on the limiting shear stress model. According to the distribution of the interfacial shear stress and the fluid pressure, the surface slip property is optimized so that a maximum hydrodynamic load support can be obtained. The surface slip property and the size of the slip zone are a function of the location coordinate. Numerical analysis of 2-D slip flow is more complicated than 1-D slip flow since both of the slip magnitude and direction are unknown *a priori*. We give here a multi-linearity method for the slip control equation of 2-D wall slip. We investigate 2-D wall slip and the hydrodynamics of a finite length slider bearing with any values of the surface limiting shear stress.

1 Multi-linearity method for the slip control equation

It is supposed that the sliding (lower) surface of the slider bearing has a surface limiting shear stress high enough to inhibit wall slip, as shown in Figure 1. But the stationary (upper) surface consists of the slip zone ($\tau_L^* = 0$) and the no-slip zone. We call such a wedge with a designed slip zone the slip wedge. Suppose that the lower surface (surface *b*) moves with a velocity *U* in *x* direction. Let u_s and v_s denote respectively the slip velocity components in *x* and *y* directions on the stationary (upper) surface. The magnitude and direction of the slip velocity are determined by the magnitude

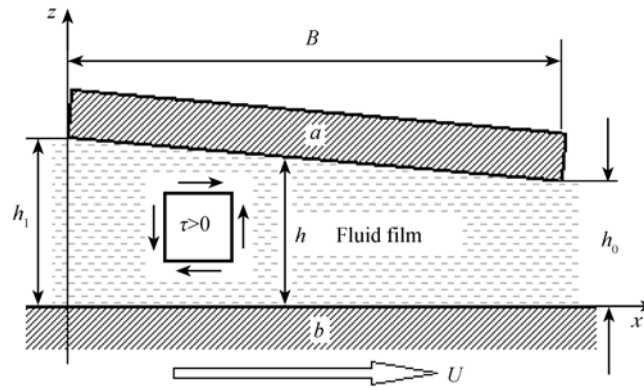


Figure 1 The schematic of geometry of a slider bearing.

and direction of the surface shear stress. If the surface shear stress components are denoted by τ_x and τ_y , the shear stress vector can be written as

$$\boldsymbol{\tau} = \tau_x \mathbf{i} + \tau_y \mathbf{j}, \quad (1)$$

where \mathbf{i} and \mathbf{j} denote the unit vectors in x and y direction respectively. If the limiting shear stress is denoted by τ_L , the surface shear stress should be within a closed set:

$$C_\infty(\tau_L) = \{\boldsymbol{\tau} : f = |\boldsymbol{\tau}| - \tau_L \leq 0\}. \quad (2)$$

Eq. (2) denotes an infinite large circular cone, as shown in Figure 2(a). If the shear stress is inside the circular cone, i.e., $|\boldsymbol{\tau}| = \tau = \sqrt{\tau_x^2 + \tau_y^2} < \tau_L$, no slip occurs. If the shear stress reaches the cone surface, i.e., $\tau = \tau_L$, a slip takes place. In the 1-D wall slip, the slip occurs either in positive x direction or in negative x direction. Therefore, either an iterative technique^[16,17,20] or a parametric quadratic programming algorithm^[11,14,15] is used for the numerical solution. For 2-D wall slip, however, the iterative technique is impossible since there are countless possible slip directions. The parametric quadratic programming algorithm cannot be realized too. Now we use the regular pyramid with N side faces, as shown in Figure 2(b), to approach the circular cone as shown in Figure 2(a). In this way, eq. (2) is replaced by a group of the multi-linearity slip control equations. The closed set can be approximately written as

$$C_N(\tau_L) = \{\boldsymbol{\tau} : f_i = \tau_x \cos \beta_i + \tau_y \sin \beta_i - \zeta \leq 0, \quad i = 1, 2, \dots, N\} \quad (3)$$

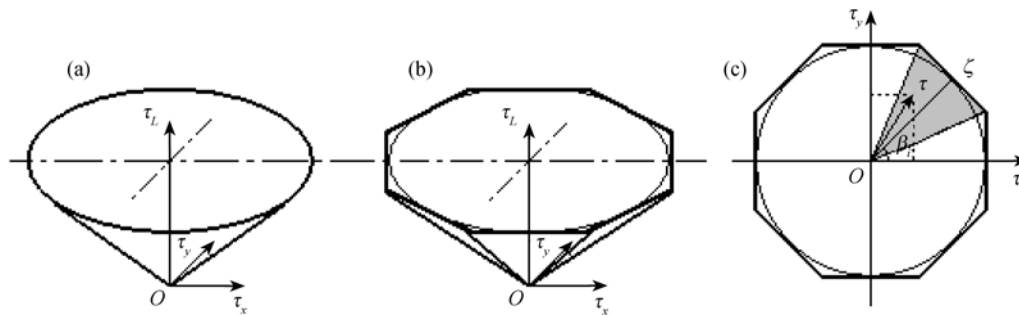


Figure 2 The constitutive model of slip control equations.

with the limit case

$$\lim_{N \rightarrow \infty} C_N(\tau_L) = C_\infty(\tau_L), \quad (4)$$

where

$$\beta_i = \frac{2\pi}{N}(i-1), \quad i=1, 2, \dots, N. \quad (5)$$

ζ is the distance from the center of the polygon (cross section of the pyramid) to the polygon side (see Figure 2(c)). The regular pyramid can be either a circumscribed pyramid or an inscribed pyramid or any other one. In the present paper, an amended pyramid dominating the same volume as the circular cone is used ($\zeta = \sqrt{(\pi/N)/\tan(\pi/N)} \tau_L$), giving the highest approximation compared with the former two. Therefore, a group of the linear slip-control equations can be obtained:

$$f_i = \tau_x \cos \beta_i + \tau_y \sin \beta_i - \zeta \leq 0, \quad i=1, 2, \dots, N. \quad (6)$$

The upper surface shear stress components are [14,15]:

$$\tau_x = \frac{h}{2} \frac{\partial p}{\partial x} + \frac{u_s - U}{h} \eta, \quad (7a)$$

$$\tau_y = \frac{h}{2} \frac{\partial p}{\partial y} + \frac{v_s}{h} \eta. \quad (7b)$$

Because the slip velocity at the stationary surface always gives a negative sign with the fluid shear stress, the slip velocity can be written as

$$u_s = \sum_{i=1}^N \lambda_i \cos(\pi + \beta_i), \quad v_s = \sum_{i=1}^N \lambda_i \sin(\pi + \beta_i) \quad (i=1, 2, \dots, N), \quad (8)$$

where λ_i is the magnitude of the possible slip velocity caused by the shear stress in β_i direction. Combining eqs. (6–8) and introducing a slack variable γ_i , we have the following general expression of the slip control equations:

$$f_\alpha^{(i)}(p, \partial p / \partial x, h, \lambda_1, \lambda_2, \dots, \lambda_N) + \gamma_i = 0, \quad (9a)$$

$$\lambda_i \cdot \gamma_i = 0, \quad \lambda_i \geq 0, \quad \gamma_i \geq 0 \quad (i = 1, 2, \dots, N). \quad (9b)$$

2 Variational principle of 2-D wall slip

The modified Reynolds equation for the slider bearing system as shown in Figure 1 can be written as [14,15,21]

$$\nabla \cdot \left(\frac{h^3}{12\eta} \nabla p \right) = \nabla \cdot \left[\frac{h}{2} (u_s + U) \mathbf{i} + \frac{h}{2} v_s \mathbf{j} \right] + \frac{\partial h}{\partial t}. \quad (10)$$

For a steady flow, the variational function for eq. (10) is

$$J(p) = \int_A \left\{ \left[\frac{h^3}{24\eta} \nabla p - \frac{h}{2} ((U + u_s) \mathbf{i} + v_s \mathbf{j}) \right] \cdot \nabla P \right\} dA + \int_{S_q} q_s p_s ds, \quad (11)$$

where A is the domain area of the bearing system, q_s the known boundary volume flow, p_s the unknown fluid pressure corresponding to q_s . Making variational operation for eq. (11) under control of eq. (9) together with the finite element technique and quadratic programming algorithm, we

can obtain both the fluid pressure and wall slip in one solution step^[22].

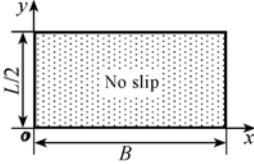
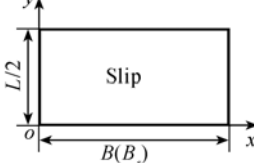
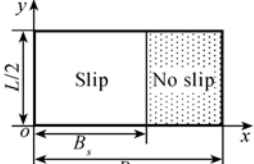
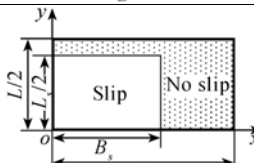
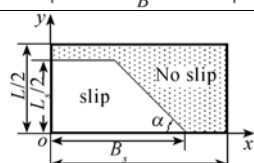
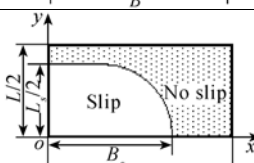
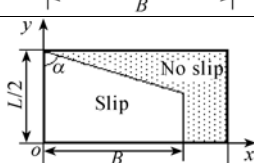
3 Computation and optimization results

For the finite slider bearing, as shown in Figure 1, L and B denote the length and width of the bearing respectively. In this paper, the case of $L/B=1$ is studied. Surface a is a complex surface consisting of two zones with no-slip and perfect slip (zero limiting shear stress), i.e., a so-called ‘slip wedge’. A maximum hydrodynamic load support can be obtained by adjusting some geometrical parameters, such as the shape and size of the slip zone at surface a . Strictly speaking, this is a topology optimization problem with a very big mathematical difficulty. For simplicity, however, we carry out a parametric optimization in the present paper. We first give several simple shapes of the slip zone, and then find the maximum hydrodynamic load support by optimizing the geometry size of the slip zone. By taking advantage of the x -axial symmetry, half of the bearing is analyzed. The studied domain is meshed by linearity triangle elements. The following non-dimensional parameters are used in this paper: dimensionless limiting shear stress, $\tau_L^* = (h_0/U\eta)\tau_L$; dimensionless hydrodynamic fluid film press, $p^* = (h_0^2/U\eta B)p$; dimensionless friction drag in x direction, $F^* = (h_0/U\eta BL)F$; dimensionless friction coefficient, $\mu^* = F^*/W^* = \mu \frac{B}{h}$, where the superscript symbol $*$ denotes the dimensionless parameter but the corresponding parameter without the star $*$ denotes the dimensional value. The convergence ratio ξ is defined as $\xi = h_1/h_0 - 1$.

Table 1 lists several profiles of the slip zone at the stationary surface (surface a) and the optimization results, where the subscript c denotes the classical no-slip solution, max denotes the optimal value, s denotes the slip solution. The optimized geometrical parameters of the slip zone were obtained at $\xi = 1$. It can be found that, for the classical no-slip slider bearing (see Table 1-I), the maximum load support $W_{c-\max}^* = 0.0698$ is obtained while $\xi = 1.3$. If the slip occurs at the entire surface (see Table 1-II), the maximum load support, $W_{s-\max}^*$, is half of the value of $W_{c-\max}^*$ while $\xi = 1.3$. For the optimized slip wedge, a higher optimal load support can be acquired. Especially, when the slip zone looks like a trapezium (as shown in Table 1-VII), $W_{s-\max}^* = 0.1743$, which is 2.5 times the value of $W_{c-\max}^*$. Even if surface a is simply separated into two parts in x direction (see Table 1-III), $W_{s-\max}^*$ equals 0.1218, which is 1.74 times the value of $W_{c-\max}^*$. As for the friction drag in x direction, Table 1 shows that almost the same friction drag is obtained corresponding to the maximum load support for the classical slider bearing and the optimized slip wedge. Due to the higher hydrodynamic load support, the optimized slip wedge always has a lower friction coefficient than that of the classical slider bearing. In other words, compared with the traditional geometry wedge, the slip wedge can get a higher hydrodynamic load support, but has a lower friction coefficient. It should be pointed out that when ξ equals zero the slip wedge has the maximum load support. However, for the traditional slider bearing, no fluid load support exists when $\xi = 0$ ^[23].

In order to discuss the effect of the convergence ratio, ξ , on the hydrodynamic load support and

Table 1 The geometry size, optimal hydrodynamic load support, friction drag and the friction coefficient of a slip wedge compared with the traditional no-slip gap^{a)}

| No. | Geometry of slip zone | Optimal slip zone | Optimal convergent ratio | Hydrodynamic force, friction drag and friction coefficient | Comparison with traditional optimal results |
|-----|---|---|--------------------------|--|--|
| I |  | / | $\xi \approx 1.3$ | $W_{c-\max}^* = 0.0698$ $F_c^* = 0.6634$ $\mu_c^* = 9.504$ | $W_r^* = 1$ $F_r^* = 1$ $\mu_r^* = 1$ |
| II |  | / | $\xi \approx 1.3$ | $W_{s-\max}^* = 0.0349$ $F_s^* = 0.0340$ $\mu_s^* = 0.974$ | $W_r^* = 0.5$ $F_r^* = 0.05$ $\mu_r^* = 0.1$ |
| III |  | $B_s / B \approx 0.55$ | $\xi = 0$ | $W_{s-\max}^* = 0.1218$ $F_s^* = 0.5998$ $\mu_s^* = 4.92$ | $W_r^* = 1.74$ $F_r^* = 0.9$ $\mu_r^* = 0.52$ |
| IV |  | $B_s / B \approx 0.65$ $L_s / L \approx 0.8$ | $\xi = 0$ | $W_{s-\max}^* = 0.1588$ $F_s^* = 0.6470$ $\mu_s^* = 4.074$ | $W_r^* = 2.28$ $F_r^* = 0.98$ $\mu_r^* = 0.43$ |
| V |  | $\alpha \approx 45^\circ$ $B_s / B \approx 0.8$ $L_s / L \approx 0.9$ | $\xi = 0$ | $W_{s-\max}^* = 0.1691$ $F_s^* = 0.6563$ $\mu_s^* = 3.881$ | $W_r^* = 2.42$ $F_r^* = 0.99$ $\mu_r^* = 0.41$ |
| VI |  | $B_s / B \approx 0.65$ $L_s / L \approx 0.9$ | $\xi = 0$ | $W_{s-\max}^* = 0.1699$ $F_s^* = 0.6758$ $\mu_s^* = 3.978$ | $W_r^* = 2.43$ $F_r^* = 1.02$ $\mu_r^* = 0.42$ |
| VII |  | $\alpha \approx 70^\circ$ $B_s / B \approx 0.7$ | $\xi = 0$ | $W_{s-\max}^* = 0.1743$ $F_s^* = 0.6469$ $\mu_s^* = 3.711$ | $W_r^* = 2.50$ $F_r^* = 0.98$ $\mu_r^* = 0.41$ |

a) W_r^*, F_r^*, μ_r^* are defined as $W_r^* = W_{s-\max}^* / W_{c-\max}^*$, $F_r^* = F_s^* / F_c^*$, $\mu_r^* = \mu_s^* / \mu_c^*$.

the friction drag, Figure 3 shows the relationship of W^* and F^* versus ξ , respectively. For convenience, four typical surfaces are discussed in the present paper, i.e., cases I, II, III and VII as shown in Table 1. Obviously, as shown in Figure 3(a), the convergence ratio, ξ , affects the hydrodynamic load support in two opposite ways. For the slider bearing whose stationary surface is either no-slip or perfect slip, W^* obtains the maximum value when $\xi = 1.3$. However, for the slip

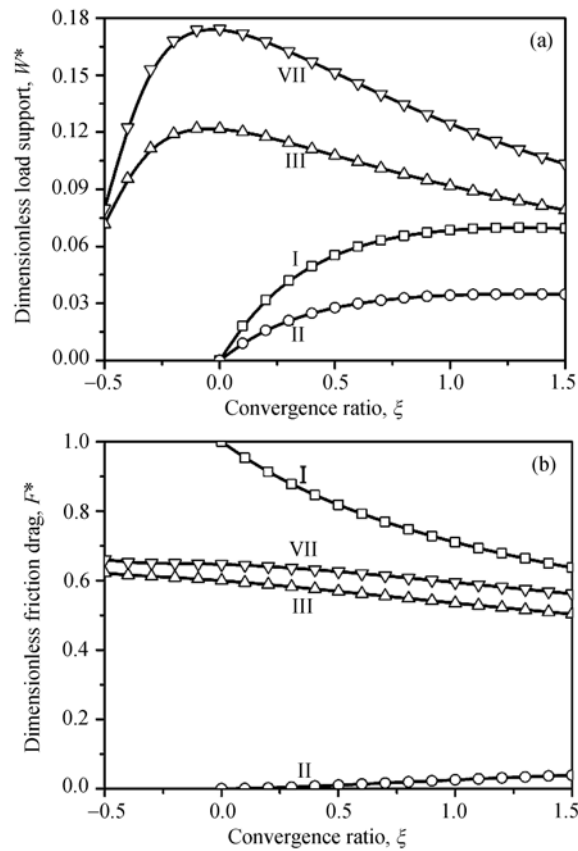


Figure 3 Comparison of the performance of the slip wedge and the no-slip wedge. (a) The optimal hydrodynamic load support; (b) the non-dimensional friction drag.

wedge, W^* increases continuously with ξ ranging from 1.5 to 0, and reaches the maximum value when $\xi = 0$. Moreover, the hydrodynamic load support of the slip wedge can maintain at a high level compared with the traditional slider bearing. This is beneficial to enhance the dynamic stability and the operation security of the slider bearing system. As shown in Figure 3(b), except for the perfect slip taking place at the entire stationary surface (slider bearing II), the lower the convergence ratio ξ , the higher the friction drag. For the same value of ξ , slider bearing II has the lowest friction drag, but slip wedges III and VII have the moderate friction drags, and the traditional slider bearing I has the highest value of the friction drag.

Figures 4(a) and (b) give the pressure distributions for the slip wedge VII with the maximum load support ($\xi = 0$) and for the traditional slider bearing when $\xi = 1.3$, respectively. Obviously, the differences between them are very big. The former gives the similar pressure distribution as the Rayleigh step bearing. The pressure gradient is not continuous at the boundary of the slip zone and the no-slip zone, where the maximum pressure occurs. Figure 5(a) gives the slip velocity field in the slip zone, where the slip velocity at the inlet gives the same direction as the sliding velocity of the lower surface. Figure 5(b) shows the volume flow in the slip wedge versus the convergence ratio ξ , while the inset gives the corresponding volume flow of the traditional slider bearing. It can be seen that volume flow in the slip wedge increases due to velocity slip at the stationary surface. However, at the two sides and the outlet, there is no wall slip to accelerate the leakage. In order to

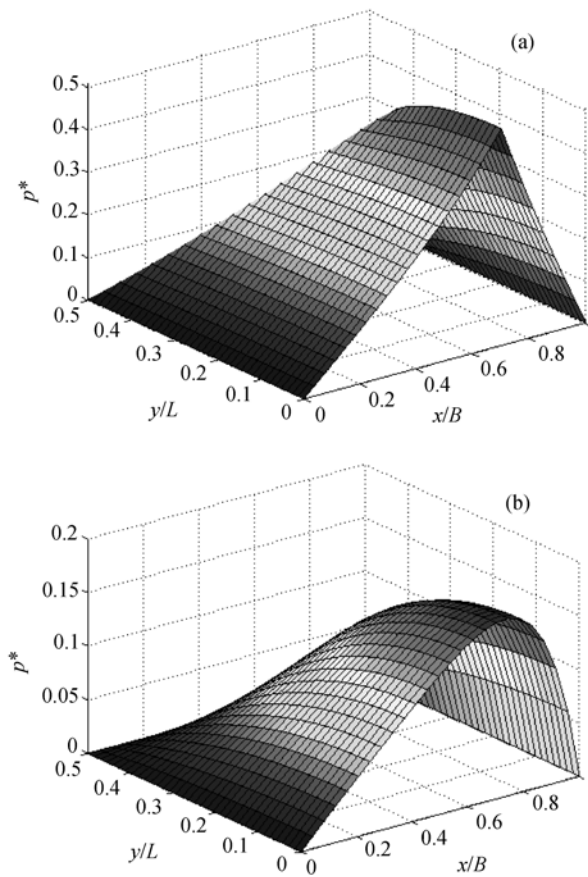


Figure 4 Pressure distributions of the slider bearing for (a) the VII slip wedge ($\xi = 0$) and (b) the traditional slider bearing ($\xi = 1.3$).

keep the volume continuity, the system has to build up a high pressure to accelerate the leakage. This can explain why slip wedge III gives the lower fluid load support than the other slip wedges. On one side, the slip wedge should be so designed that the inlet volume flow is increased utilizing the wall slip. On the other hand, the side leakages should be inhibited utilizing the no-slip boundary condition. Under the coupling of the two actions mentioned above, the gap flow produces a very high hydrodynamic pressure. If ξ is equal to zero, the friction drag vanishes (see Figure 3(b)) while a perfect slip occurs at the entire stationary surface. In other words, a perfect slip can give rise to a low friction drag. Because the perfect slip occurs at a big domain of the slip wedge, as a whole, a small value of the friction drag is obtained and thus the friction coefficient is kept at a very low level.

4 Discussion

This paper mainly studied the hydrodynamics of a slip wedge consisting of the no-slip zone and the slip zone with a zero limiting shear stress. We have also studied the hydrodynamics of the optimized slip wedge when the limiting shear stress at the slip zone is considerably large. It was found that with the increase of the limiting shear stress, the hydrodynamic effect decreases and finally reaches the level of the traditional no-slip solution. The limiting shear stress was found to depend

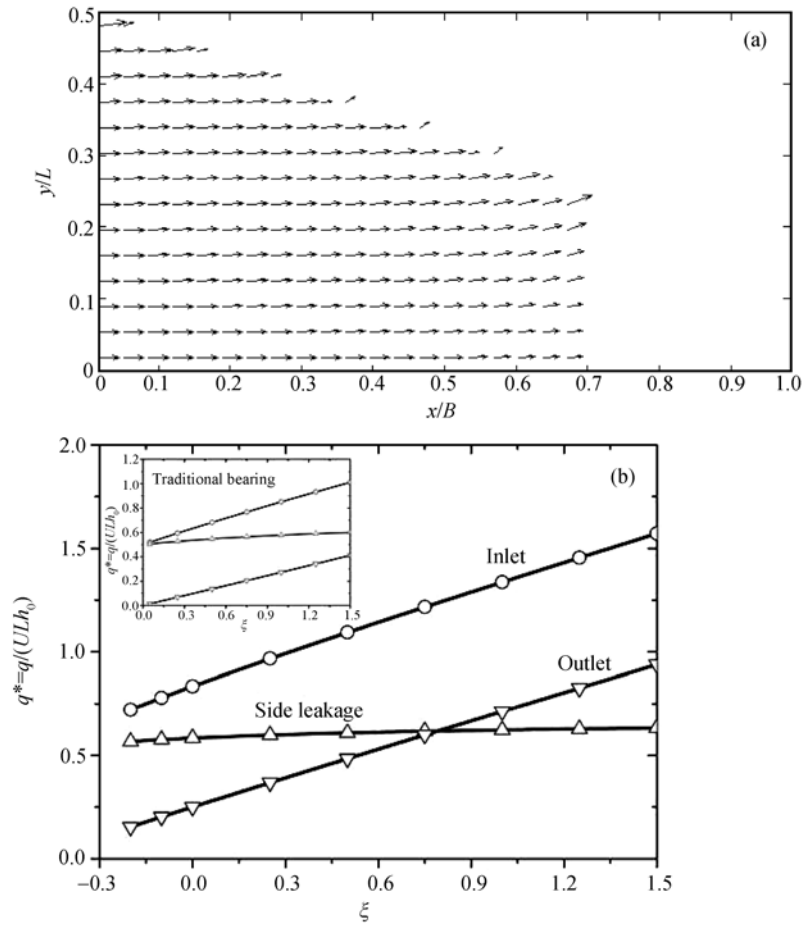


Figure 5 (a) Slip velocity field when slip wedge VII obtains its highest hydrodynamic load support; (b) volume flow versus convergence ratio.

on surface roughness, wettability, fluid viscosity, nanobubbles, etc., among which surface wettability and roughness were considered as the two important effect factors. Wettability describes the surface interaction of the moleculars of the solid and liquid. Usually the better the surface wettability, the higher the surface limiting shear stress. The reported limiting shear stress of the wetting interface of oil and steel is very large, ranging from 0.16 to 8 MPa^[15]. However, the surface limiting shear stress of the ultrahydrophilic surface is as low as 0.33 Pa^[7-9,11], which can be considered as a perfect slip surface. In one word, the worse the wettability, the larger the slip. However, there are two opposite opinions for the roughness effect on slip. Pit et al.^[3] and Granick et al.^[6] reported that roughness inhibits the slip, but Bonaccorso et al.^[24] and Craig et al.^[5] reported that roughness increases the slip. Surface limiting shear stress can be controlled by many methods, but at the present time the chemical method (controlling wettability) and machining method (controlling roughness) are usually used.

We can also change the slip property of the moving surface in order to change the hydrodynamics of the slip gap. But we find that if the limiting shear stress on the moving surface is decreased to a level that a slip occurs at, the hydrodynamic response will decrease very much. However, if the moving surface is designed as a composite slip surface, the system is in an unsteady

state and no great significance exists in engineering applications.

5 Conclusions

This paper presents the concept of the slip wedge. It is shown that controlling the shape and size of the slip zone can give many advanced properties for the slip wedge compared with the traditional no-slip gap. The main conclusions can be summarized as follows:

(1) The slip wedge can give rise to more than twice (with a maximum 2.5 times) the hydrodynamic load support as large as the traditional no-slip gap.

(2) The slip wedge usually gives a large fluid load support, but gives a low friction drag.

(3) Generally speaking, a slip wedge obtains its highest hydrodynamic pressure in a parallel slip gap. The hydrodynamic load support is not so sensitive to the convergent ratio, which is helpful to improve the operation stability of the system.

- 1 Reynolds O. On the theory of lubrication and its application to Mr Beauchamp Tomer's experiments, including an experimental determination of the viscosity of olive oil. *Phil Trans Roy Soc*, 1886, 177: 157–167
- 2 Cameron A. The viscosity wedge. *ASLE Trans*, 1958, 1: 248–253
- 3 Pit R, Hervet H, Leger L. Direct experimental evidence of slip in hexadecane: Solid interfaces. *Phys Rev Lett*, 2000, 85: 980–983[DOI]
- 4 Hervet H, Leger L. Flow with slip at wall: From simple to complex fluids. *C R Physique*, 2003, 4: 241–249[DOI]
- 5 Craig V S J, Neto C, Williams R M. Shear-dependent boundary slip in an aqueous Newtonian liquid. *Phys Rev Lett*, 2000, 87: 054504[DOI]
- 6 Zhu Y X, Granick S. Rate-dependent slip of Newtonian liquid at smooth surfaces. *Phys Rev Lett*, 2001, 87: 096105[DOI]
- 7 Zhu Y X, Granick S. Limits of the hydrodynamic no-slip boundary condition. *Phys Rev Lett*, 2002, 88: 106102[DOI]
- 8 Zhu Y X, Granick S. No-slip boundary condition switches to partial slip when fluid contains surfactant. *Langmuir*, 2002, 18: 10058–10063
- 9 Granick S, Zhu Y X, Lee H. Slippery questions about complex fluids flowing past solids. *Nat Mater*, 2003, 2: 221–227[DOI]
- 10 Kassner M E, Nemat-Nasser S, Suo Z, et al. New directions in mechanics. *Mech Mater*, 2005, 37: 231–259[DOI]
- 11 Wu C W, Ma G J. On the boundary slip of fluid flow. *Sci China Ser G-Phys Mech Astron*, 2005, 48: 178–187
- 12 Thompson P R, Troian S M. A general boundary condition for fluid flow at solid surfaces. *Nature*, 1997, 389: 360–362
- 13 Wang H, Hu Y Z, Zhou K, et al. Nano-tribology through molecular dynamics simulations. *Sci China Ser A-Math*, 2001, 44: 1049–1055
- 14 Wu C W, Ma G J. Abnormal behavior of a hydrodynamic lubrication journal bearing caused by wall slip. *Tribol Int*, 2005, 38: 492–499[DOI]
- 15 Wu C W, Ma G J, Sun H S. Viscoplastic lubrication analysis in a metal-rolling inlet zone using parametric quadratic programming. *ASME J Tribol*, 2005, 127: 605–610[DOI]
- 16 Spikes H A. The half-wetted bearing (I): Extended Reynolds equation. *Proc Instn Mech Engrs, Part J: J Eng Tribol*, 2003, 217: 1–14
- 17 Spikes H A. The half-wetted bearing (II): Potential application in low load contacts. *Proc Instn Mech Engrs, Part J: J Eng Tribol*, 2003, 217: 15–26
- 18 Salant R F, Fortier A E. Numerical analysis of a slider bearing with a heterogeneous slip/no-slip surface. *Tribol Trans*, 2004, 47: 328–334[DOI]
- 19 Spikes H, Granick S. Equation for slip of simple liquids at smooth solid surfaces. *Langmuir*, 2003, 19: 5065–5071[DOI]
- 20 Stahl J, Jacobson B O. A lubricant model considering wall-slip in EHL line contacts. *ASME J Tribol*, 2003, 125: 523–532[DOI]
- 21 Huebner K H. *The Finite Element Method for Engineers*. New York: Wiley, 1975
- 22 Zhong W X, Zhang H W, Wu C W. *Parametric Variational Principle and Engineering Applications*. Beijing: Science Press, 1997
- 23 Cameron A. *Basic Lubrication Theory*. 3rd ed. Chichester: Ellis Horwood Ltd, 1981
- 24 Bonaccorso E, Kappl M, Butt H J. Hydrodynamic force measurements: Boundary slip of hydrophilic surfaces and electrokinetic effects. *Phys Rev Lett*, 2002, 88: 076103[DOI]